PHYSICAL REVIEW E VOLUME 54, NUMBER 4 OCTOBER 1996

Rayleigh-Taylor instability in finite-thickness fluids with viscosity and surface tension

Karnig O. Mikaelian
University of California, Lawrence Livermore National Laboratory, Livermore, California 94550

(Received 10 October 1995; revised manuscript received 4 April 1996)

We consider the Rayleigh-Taylor instability in two finite-thickness fluids including the effects of viscosity and surface tension. The eight equations expressing boundary, continuity, and jump conditions imposed on the eigenfunction are written in the form $MV=0$ where M is an 8×8 matrix and V is a vector containing the eight coefficients that appear in the eigenfunction. Exact numerical results are obtained by solving $\det(M)=0$, the dispersion relation which determines the growth rate γ as a function of the physical parameters of the system. For the case of a semi-infinite viscous fluid with a free surface the exact result is given analytically. We also derive an approximate analytic formula for arbitrary thicknesses, compare it with the exact results, and briefly discuss recent experiments on finite-thickness fluids. [S1063-651X(96)07310-2]

PACS number(s): 47.20.−k, 52.35.Py, 47.40.Nm

I. INTRODUCTION

In this paper we consider the Rayleigh-Taylor instability in finite-thickness fluids including the effects of viscosity and surface tension. The system consists of two fluids of densities ρ_1 and ρ_2, thicknesses t_1 and t_2, viscosities μ_1 and μ_2, and surface tension $T^{(s)}$ between the two fluids. Perturbations of wave number k at the interface of the two fluids grow exponentially in time with a growth rate γ if the acceleration g is directed from the low-density (ρ_1) fluid towards the high-density (ρ_2) fluid. The goal is to obtain the dispersion relation that gives γ as a function of the other nine variables of the system.

Earlier work [1] has focused primarily on semi-infinite fluids, i.e., $t_1=t_2=\infty$, which is a considerably simpler system than the finite-thickness case. Even then the exact solutions must be obtained numerically. An approximate dispersion relation for such semi-infinite fluids was derived recently [2]

$$\gamma^2+2k^2\nu\gamma-gkA\left(1-\frac{k^2}{k_c^2}\right)=0, \tag{1}$$

where the Atwood number $A=(\rho_2-\rho_1)/(\rho_2+\rho_1)$, $\nu=(\mu_2+\mu_1)/(\rho_2+\rho_1)$, and $k_c=[(\rho_2-\rho_1)g/T^{(s)}]^{1/2}$. Equation (1), without the surface tension term, was first proposed by Bellman and Pennington [3] and subsequently by Hide [4], though his derivation was criticized by Reid [5] (see Ref. [1] for historical remarks). In this paper we present exact numerical solutions to the finite-thickness case and an approximate analytic dispersion relation that generalizes Eq. (1) to finite-thickness fluids.

There are two motivations for this extension: Microgravity experiments have been carried out [6] where both viscosity and surface tension are present in finite-thickness fluids, and the results compared with a dispersion relation that contains the effect of finite thickness and surface tension only

$$\frac{\gamma^2}{gk}=\frac{\rho_2-\rho_1-k^2T^{(s)}/g}{\rho_2\coth(kt_2)+\rho_1\coth(kt_1)} \tag{2}$$

[Eq. (10) in Ref. [7]], presumably because there is no formula containing all three effects of finite thickness, surface tension, and viscosity. Unlike Eq. (1), Eq. (2) is an exact result. The second motive is that the steps in our treatment are quite general and can be applied to other problems requiring finite-thickness corrections.

The exact (but numerical) results are given in Sec. II. The approximate (but analytic) results are given in Sec. III, where we also discuss recent experiments [6]. In the course of this investigation we have derived an *exact and analytic* solution for the case $T^{(s)}=0$, $\rho_1=0$, and $t_2=\infty$. As far as we know this is the only exact analytic expression for a viscous fluid valid for all wave numbers, and naturally we use it to test our numerical results and approximate expressions. The derivation is detailed in the Appendix.

II. EXACT RESULTS

Our starting point is the general eigenvalue equation, Eq. (41) in Ref. [1]:

$$\begin{aligned}&D\left[\left(\rho-\frac{\mu}{\gamma}(D^2-k^2)\right)DW-\frac{1}{\gamma}D\mu(D^2+k^2)W\right]\\&+k^2\left[\frac{g}{\gamma^2}D\rho-\frac{k^2}{\gamma^2}\sum_i T_i^{(s)}\delta(y-y_i)\right]W\\&-k^2\left[\rho-\frac{\mu}{\gamma}(D^2-k^2)\right]W+2\frac{k^2}{\gamma}D\mu DW=0,\end{aligned} \tag{3}$$

where $W(y)$ is the perturbed velocity and $D\equiv d/dy$, $\hat{y}$ being the direction of the constant acceleration g.

Integrating Eq. (3) we obtain

$$\begin{aligned}&\gamma^2\int\rho W\,dy+k^2\sum_i T_i^{(s)}W(y_i)+\gamma\int\mu(D^2+k^2)W\,dy\\&\quad-g\int D\rho\,W\,dy\\&\quad=\Delta\left\{2\gamma\mu DW+\frac{\gamma^2}{k^2}\left[\rho-\frac{\mu}{\gamma}(D^2-k^2)\right]DW\right.\\&\qquad\left.-\frac{\gamma}{k^2}D\mu(D^2+k^2)W\right\},\end{aligned} \tag{4}$$

1063-651X/96/54(4)/3676(5)/$10.00

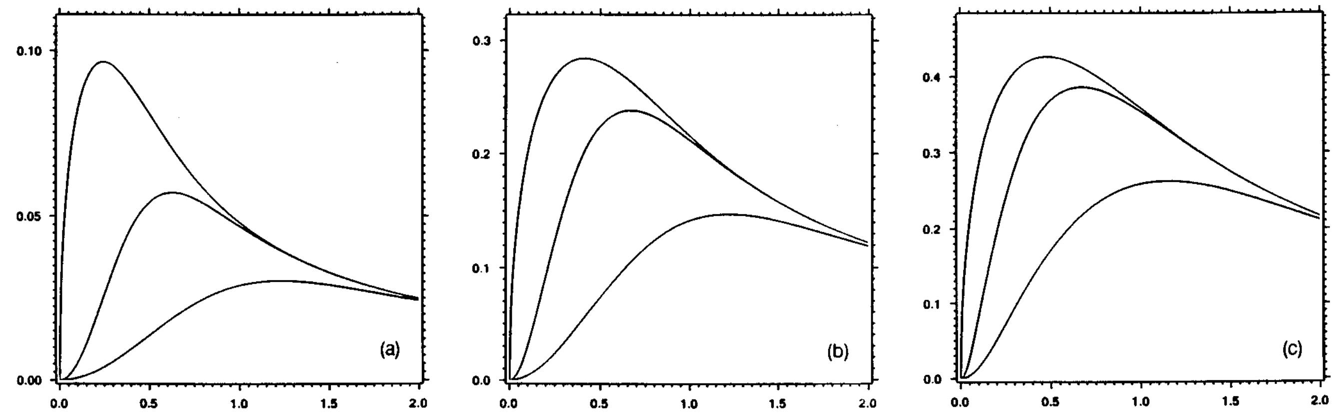

FIG. 1. Y vs X for the case $T^{(s)}=\Delta\nu=0$, $H_1=H_2=H$. In each diagram the uppermost, middle, and lowest curves correspond to $H=200$, 4, and 2, respectively. The Atwood number A is 0.1, 0.5, and 0.9 in diagrams (a), (b), and (c), respectively. These curves are obtained by numerically solving Eq. (17).

where $\Delta(f)\equiv f(t_2)-f(-t_1)$. The left-hand-side (lhs) of Eq. (4) is identical to the lhs of Eq. (4) in Ref. [2]. The right-hand-side (rhs) represents the ''surface terms'' that were dropped in Ref. [2]. We emphasize that Eqs. (3) and (4) are exact, general, and apply to fluids of arbitrary density profile $\rho(y)$ and viscosity profile $\mu(y)$ in the region $-t_1\leqslant y\leqslant t_2$.

We now specialize to the case of two constant-density and constant-viscosity fluids, i.e.,

$$\rho=\rho_1,\quad \mu=\mu_1,\quad -t_1\leqslant y\leqslant 0, \tag{5a}$$

$$\rho=\rho_2,\quad \mu=\mu_2,\quad 0\leqslant y\leqslant t_2. \tag{5b}$$

It is straightforward to show that for the *inviscid* case (i.e., $\mu_1=\mu_2=0$) the exact eigenfunctions are

$$W=\frac{\sinh(kt_1+ky)}{\sinh(kt_1)},\quad -t_1\leqslant y\leqslant 0, \tag{6a}$$

$$W=\frac{\sinh(kt_2-ky)}{\sinh(kt_2)},\quad 0\leqslant y\leqslant t_2. \tag{6b}$$

For the viscous case, however, the exact eigenfunctions are more complicated:

$$W=A_1e^{ky}+B_1e^{q_1y}+C_1e^{-ky}+D_1e^{-q_1y},\quad -t_1\leqslant y\leqslant 0, \tag{7a}$$

$$W=A_2e^{-ky}+B_2e^{-q_2y}+C_2e^{ky}+D_2e^{q_2y},\quad 0\leqslant y\leqslant t_2, \tag{7b}$$

where

$$(q_{1,2})^2=k^2+\gamma\frac{\rho_{1,2}}{\mu_{1,2}}, \tag{8}$$

and $q_{1,2}$ are defined such that their real parts are positive. Our notation follows that of Chandrasekhar [1] who gave Eq. (7) with $C_1=D_1=C_2=D_2=0$ because he considered $t_1=t_2=\infty$.

The following eight equations determine the eight constants A_1 through D_2:

$$A_1+B_1+C_1+D_1=A_2+B_2+C_2+D_2, \tag{9}$$

$$kA_1+q_1B_1-kC_1-q_1D_1=-kA_2-q_2B_2+kC_2+q_2D_2, \tag{10}$$

$$A_1e^{-kt_1}+B_1e^{-q_1t_1}+C_1e^{kt_1}+D_1e^{q_1t_1}=0, \tag{11}$$

$$A_2e^{-kt_2}+B_2e^{-q_2t_2}+C_2e^{kt_2}+D_2e^{q_2t_2}=0, \tag{12}$$

$$A_1ke^{-kt_1}+B_1q_1e^{-q_1t_1}-C_1ke^{kt_1}-D_1q_1e^{q_1t_1}=0, \tag{13}$$

$$-A_2ke^{-kt_2}-B_2q_2e^{-q_2t_2}+C_2ke^{kt_2}+D_2q_2e^{q_2t_2}=0, \tag{14}$$

$$\begin{aligned}&\mu_1[2k^2(A_1+C_1)+(q_1^2+k^2)(B_1+D_1)]\\&\quad=\mu_2[2k^2(A_2+C_2)+(q_2^2+k^2)(B_2+D_2)],\end{aligned} \tag{15}$$

$$\begin{aligned}&(A_2-C_2)\rho_2+(A_1-C_1)\rho_1+\frac{gk}{\gamma^2}(\rho_1-\rho_2+k^2T^{(s)}/g)\\&\times(A_1+B_1+C_1+D_1)+2\frac{k}{\gamma}(\mu_1-\mu_2)\\&\times(kA_1+q_1B_1-kC_1-q_1D_1)=0.\end{aligned} \tag{16}$$

Equations (9) and (10) follow from the continuity of $W(y)$ and $DW(y)$ at $y=0$. Equations (11) and (12) express $W(y)=0$ at $y=-t_1$ and $y=t_2$, respectively. Equations (13) and (14) express $DW(y)=0$ at $y=-t_1$ and $y=t_2$ respectively. Equation (15) expresses the continuity of $\mu(D^2+k^2)W(y)$ at $y=0$. And, finally, Eq. (16) is the jump condition which $W(y)$ must satisfy at $y=0$ [see Eq. (40) in Ref. [1]].

Equations (9)–(16) can be written in the form $MV=0$, where M is an 8×8 matrix and V is a vector having the eight constants A_1 through D_2 as its elements. A nontrivial solution is obtained only if

$$\mathrm{Det}(M)=0 \tag{17}$$

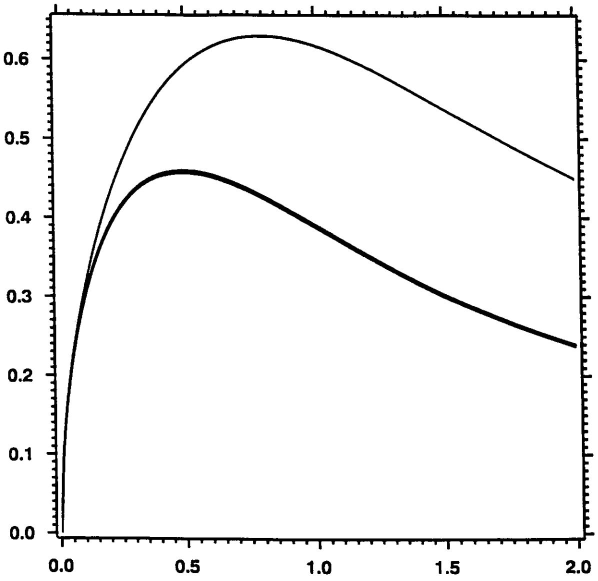

FIG. 2. Y vs X for the case of a semi-infinite viscous fluid with a free surface ($A=1$) and no surface tension. Three curves are plotted in this figure: The analytic result given by Eqs. (21)–(23); the numerical solution to Eq. (17) with $H_1=H_2=200$, and $A=0.99$ (this curve lies almost exactly on top of the first curve); and the approximate result, Eq. (24), which is above the other two.

and this equation determines the growth rate γ or, equivalently, $q_{1,2}$. In other words Eq. (17) is the dispersion relation. It must be solved numerically.

Following Chandrasekhar [1] we plot Y as a function of X where Y is the dimensionless growth rate

$$Y=\gamma(\nu/g^2)^{1/3} \tag{18a}$$

and X is the dimensionless wave number

$$X=k(\nu^2/g)^{1/3}. \tag{18b}$$

An analysis of Eqs. (9)–(16) reveals that Y depends only on the six independent variables X, A, $T^{(s)}$, $\Delta\nu$, H_1, and H_2, where $\Delta\nu=\nu_2-\nu_1=\mu_2/\rho_2-\mu_1/\rho_1$ and

$$H_i=t_i(g/\nu^2)^{1/3}, \quad i=1,2. \tag{19}$$

Our numerical examples concentrate on $H_1=H_2=H$. Furthermore, we take $T^{(s)}=\Delta\nu=0$, so that $\nu_1=\nu_2=\nu$. The six variables are thus reduced down to three, i.e., $Y=Y(X,A,H)$, and we plot Y as a function of X for various values of A and H. For $H=\infty$ our results must agree with the curves given by Chandrasekhar (Figs. 106 and 107 in Ref. [1]).

In Fig. 1 we plot Y vs X for $A=0.1$, 0.5, and 0.9, taking $H=2$, 4, and 200 for each value of A. The range of A covers low, intermediate, and high values of the Atwood number, while the range of H covers low to high viscosity fluids. For example, $\nu_{\text{water}}\approx 10^{-2}$ cm^2/s and, taking $t\approx 1$ cm, $g=980$ cm/s^2, we have $H\approx 200$. Glycerine, on the other hand, has $\nu_{\text{glycerine}}\approx 10$ cm^2/s, hence $H\approx 2$.

For fixed ν varying H corresponds to varying the thickness of the fluids. We may consider $H=200$ close to the semi-infinite ($H=\infty$) case for which prior numerical results are available, and indeed the $H=200$ curves in Figs. 1(a), 1(b), and 1(c) are in close agreement with curves 3, 6, and 7 in Figs. 106 and 107 in Ref. [1] corresponding to $A=0.1$, 0.5, and 0.9, respectively.

Figure 1 shows that, *at any value of A*, decreasing H decreases Y and moves the peak to larger X, i.e., larger k (smaller wavelength λ, since $k=2\pi/\lambda$). In addition, Fig. 1 shows that by $X\approx 2$ the growth rate has become insensitive to thickness H, since we see in Fig. 1 that the three curves for $H=2$, 4, and 200 coalesce into one curve by $X\approx 2$. This is expected on physical grounds since shorter-wavelength perturbations are more localized near the interface and are insensitive to how far the fluids extend. Note that the coalescence occurs far all values of A.

If $T^{(s)}\neq 0$ then Eqs. (9)–(16) show that $\gamma=0$ when $k=k_c$. As Chandrasekhar points out [1] $\gamma=0$ when $k=k_c$ for any value of the viscosities μ_1 and μ_2. Our analysis shows that this zero is not only independent of μ_1 and μ_2, but of t_1 and t_2 as well.

Equations (9)–(16) reduce to the four equations given in Ref. [1] for $t_1=t_2=\infty$: Set $C_1=D_1=C_2=D_2=0$ and delete Eqs. (11)–(14). M becomes a 4×4 matrix and Eq. (17) becomes a quartic equation that is still too complicated to be solved analytically. However, if we set $A=1$ and $T^{(s)}=0$, we obtain

$$Z^4+2Z^2-4Z+1-Q=0, \tag{20}$$

where

$$Z\equiv q_2/k=\sqrt{1+Y/X^2}, \quad Q\equiv 1/X^3. \tag{21}$$

This is the simplest Rayleigh-Taylor problem with viscosity: A semi-infinite fluid with a free surface. Equation (20) agrees with Eq. (125) of Ref. [1] after we set $\alpha_2=1$, $\alpha_1=0$ in that equation $[\alpha_{2,1}\equiv 0.5(1\pm A)]$.

The solution to Eq. (20) is (details are given in the Appendix)

$$Z=\frac{e+\sqrt{e^2-4(d-f)}}{2}, \tag{22}$$

where

$$d=\tfrac{1}{3}+(Q/3+\tfrac{19}{27}+\sqrt{P})^{1/3}+(Q/3+\tfrac{19}{27}-\sqrt{P})^{1/3}, \tag{23a}$$

$$f=\sqrt{d^2+Q-1}, \tag{23b}$$

and

$$e=2/f \tag{23c}$$

with

$$P=(Q^3-Q^2+18Q+11)/27. \tag{23d}$$

The dispersion relation $Y(X)$ is completely specified via Eqs. (21)–(23), and is plotted in Fig. 2. Figure 2 also contains our numerical solution to Eq. (17), i.e., the same algorithm that generated the curves in Fig. 1, with $A=0.99$ and $H=200$. We see that this numerical solution is almost identical to the analytic answer given above.

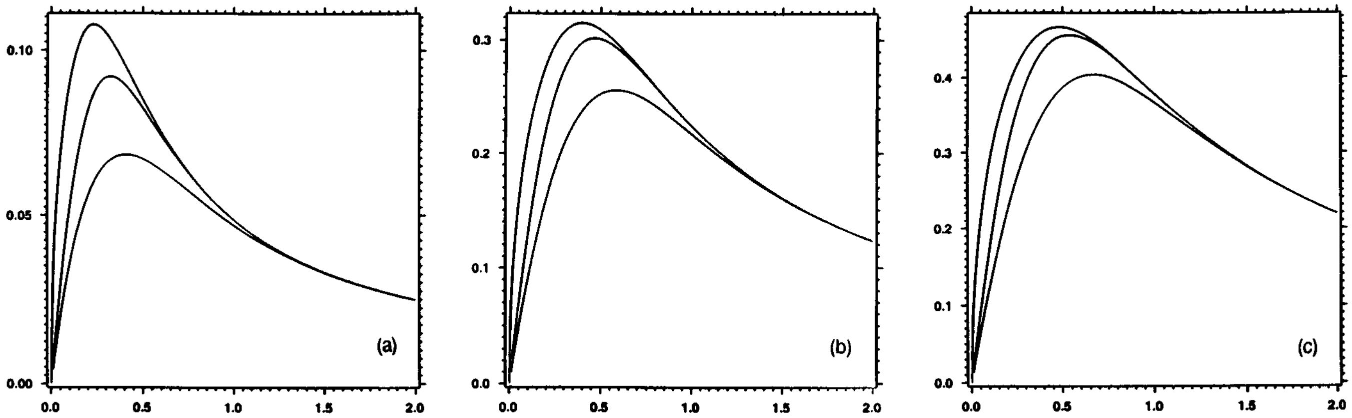

FIG. 3. Same as Fig. 1, using the approximate formula Eq. (25).

Figure 2 contains a third curve quite distinct from the other two. This is the approximate result, Eq. (1), with $T^{(s)}=0$ and $A=1$, which reads $Y^2+X^2Y-X=0$. The third curve plotted in Fig. 2 is

$$Y=\frac{-X^2+\sqrt{X^4+4X}}{2}. \tag{24}$$

We see that this solution agrees with the exact solution at small X and somewhat overestimates Y at large X. Further comparisons between exact and approximate results are given in Sec. III.

III. APPROXIMATE RESULTS

Comparisons between exact and approximate results for semi-infinite fluids, like the one shown in Fig. 2, have been made previously [3,4,8]. We should point out that the agreement is better in the presence of surface tension because both the exact result and the approximate expression, Eq. (1), go through zero at $k=k_c$, so in this sense Fig. 2 displays a worst-case comparison.

One resorts to approximate formulas to avoid numerical computation. Even for the simplest case, for which we provided an analytic solution, the approximate formula is much simpler—compare Eq. (24) with Eqs. (21)–(23). Finite-thickness fluids introduce a substantial additional complexity because the exact dispersion relation is no longer polynomial in γ because it appears in quantities like $e^{\pm q_{1,2}t_{1,2}}$—see Eqs. (11)–(14). An alternative to exact numerical results is an approximate analytic formula generalizing Eq. (1) to finite-thickness fluids, which we proceed to derive.

The extension is based on the same ''moment equation approach'' used earlier for semi-infinite fluids [2], and essentially consists of using an approximate eigenfunction in the exact moment equation, Eq. (4). Two elements are needed for this extension: First, we need to keep the ''surface terms'', i.e., the rhs of Eq. (4). Second, we need to use eigenfunctions that vanish at the boundaries $y=-t_1$ and $y=t_2$ in the frame where $y=0$ marks the interface. The inviscid eigenfunction given in Eq. (6) satisfies this condition. While Eq. (4) is exact, the approximation comes in using the inviscid eigenfunction, Eq. (6), instead of the exact eigenfunction, Eq. (7), in evaluating the integrals and the surface terms of Eq. (4). Note the substantial ''advantage'' of the inviscid Ws: they do not contain γ, hence the dispersion relation obtained by substituting Eq. (6) in Eq. (4) is guaranteed to be polynomial in γ.

An interesting point comes up when we examine the ''surface terms'' given in the rhs of Eq. (4). They contain W, DW, D^2W, and D^3W evaluated at the boundaries. The exact Ws must satisfy $W=DW=0$ on the boundaries, so one might be tempted to drop them. However, since we wish to use the approximate and inviscid eigenfunctions of Eq. (6) which satisfy only $W=0$ on the boundaries, we *cannot* drop the DW terms.

We now substitute Eq. (6) into Eq. (4) and use $\rho=\rho_1$, $\mu=\mu_1$ for $-t_1\leqslant y\leqslant 0$, and $\rho=\rho_2$, $\mu=\mu_2$ for $0\leqslant y\leqslant t_2$. Many terms can be combined using $D^2W=k^2W$. The integrations are straightforward and the result is

$$\gamma^2+2k^2\left[\frac{\mu_2\coth(kt_2)+\mu_1\coth(kt_1)}{\rho_2\coth(kt_2)+\rho_1\coth(kt_1)}\right]\gamma+\frac{k^3T^{(s)}-gk(\rho_2-\rho_1)}{\rho_2\coth(kt_2)+\rho_1\coth(kt_1)}=0. \tag{25}$$

Some of the terms from the lhs of Eq. (4) have canceled similar terms in the rhs leading to our final result, Eq. (25).

For $t_{1,2}\to\infty$ Eq. (25) reduces to the semi-infinite result, Eq. (1). For $\mu_1=\mu_2=0$ Eq. (25) reduces to Eq. (2) which is exact because Eq. (6) is the exact eigenfunction for the inviscid problem. This serves as an important check of our calculation because Eq. (2) was derived [7] by a completely different method. Had we dropped the DW terms in the rhs of Eq. (4) this agreement would be lost. Finally, for $t_{1,2}\to\infty$ *and* $\mu_1=\mu_2=0$ Eq. (25) gives $\gamma^2/gk=(\rho_2-\rho_1-k^2T^{(s)})/(\rho_2+\rho_1)$ which agrees with Eq. (51) in Ref. [1].

To compare with the exact results we plot Y vs X in Fig. 3 for the same nine cases as in Fig. 1, using this time Eq. (25). As in Fig. 2, the approximate formula somewhat overestimates the growth rate. The general trends seen in Fig. 1, however, are well captured by Eq. (25): The growth rate Y decreases as H decreases and the peaks move to larger X. Coalescence into one curve (i.e., independence from H) occurs somewhat earlier ($X\sim 1.2$) than the exact result ($X\sim 2$). The exact results (Fig. 1) indicate that before coalescence the growth rate is quite sensitive to H and, for $X<1$, Y decreases rapidly with decreasing H (meaning, of course, that perturbations grow slower in thinner fluids.) Figure 3 also shows this decrease, but it is not quite as sensitive.

If the fluids have equal thicknesses then $t_1=t_2=t$ and Eq. (25) becomes

$$\gamma^2+2k^2\nu\gamma-gkA\left(1-\frac{k^2}{k_c^2}\right)\tanh(kt)=0, \tag{26}$$

which is Eq. (1) with A replaced by $A\ \tanh(kt)$. The experiments [6] had $t_1=t_2=2.2$ cm. Finite-thickness corrections are most important for long-wavelength perturbations that probe the density profile over longer distances and hence ''feel'' the presence of fixed boundaries more than the short-wavelength perturbations. The longest wavelength in the experiment was 19 cm, so the correction to A is $\tanh(kt)$ $\approx\tanh(0.73)\approx 0.6$, i.e., the effective Atwood number is reduced by $\sim$40%. The reduction is less for shorter wavelengths: $\sim$10% for $\lambda=9.5$ cm, and $\sim$2% for the next harmonic, $\lambda=6.3$ cm. As the wavelengths get shorter the effects of finite thickness get weaker, but of course the effects of viscosity and surface tension get stronger.

Representative values from Ref. [6] are $g\sim 150$ cm/s^2, $\nu\sim 0.15$ cm^2/s, therefore the viscous length scale $(\nu^2/g)^{1/3}\sim 0.05$ cm, so that $H\sim 40$ and $0.02\leqslant X\leqslant 0.07$ for $4.75\leqslant\lambda\leqslant 19$ cm (the experiments focused on the first four harmonics.) From Fig. 1 we conclude that the growth rate is near its inviscid limit where Eq. (25) goes over to Eq. (2). The same conclusion is reached by noting that even the shortest-wavelength perturbation observed in the experiments (4.75 cm, the fourth harmonic) is about 100 times the viscous length scale ($\sim$0.05 cm), which might explain why Eq. (2) showed good agreement with the experiments at those wavelengths [6].

ACKNOWLEDGMENT

This work was performed under the auspices of the U.S. Department of Energy by the Lawrence Livermore National Laboratory under Contract No. W-7405-ENG-48.

APPENDIX

To solve the quartic equation (20) we follow the method described in Ref. [9]. The first step is to find the resolvent R of Eq. (20) from the following equation:

$$R^3-2R^2-4(1-Q)R-8(1+Q)=0. \tag{A1}$$

Any root of this cubic equation will do. Using Cardan's solution we see that

$$R=2d \tag{A2}$$

is a solution where d was defined in Eq. (23a).

Next we find e and f from

$$(R-2)Z^2+4Z+R^2/4+Q-1=(eZ+f)^2, \tag{A3}$$

which gives f and e as defined in Eqs. (23b) and (23c), respectively. An important and useful check is the relation $e^2=R-2$ that is satisfied if and only if R is a solution of Eq. (A1).

The next step is to write Eq. (20) as a biquadratic equation,

$$(Z^2+d)^2=(eZ+f)^2; \tag{A4}$$

hence

$$Z^2+d=\pm(eZ+f) \tag{A5}$$

from which the four solutions follow immediately:

$$Z_1=\frac{e+\sqrt{e^2-4(d-f)}}{2}, \tag{A6}$$

$$Z_2=\frac{e-\sqrt{e^2-4(d-f)}}{2}, \tag{A7}$$

$$Z_{3,4}=\frac{-e\pm\sqrt{e^2-4(d+f)}}{2}. \tag{A8}$$

By studying the radical $e^2-4(d\pm f)$ we find that $Z_{3,4}$ are complex, but of course that is no reason for rejection. However, we find that $\mathrm{Re}(Z_{3,4})<0$ and this makes them unacceptable because, by definition, $Z\equiv q_2/k$ and $\mathrm{Re}(q_2)>0$. (The reader might wish to consult Chandrasekhar's discussion given on pp. 444 and 445 of Ref. [1]. Except for one point noted below we agree with his statements.) In contrast to $Z_{3,4}$, $Z_{1,2}$ are both real. Furthermore, $Z_1=\mathrm{Re}(Z_1)>0$ for all X, and this is the root we reported as the solution Z in Eq. (22). We find that $Z>1$, so that the associated growth rate Y is positive as plotted in Fig. 2 $[Y\equiv(Z^2-1)X^2]$.

Turning to Z_2 we find that it is negative and therefore unacceptable for $X<1$. For $X>1$, however, we find that Z_2 is positive and therefore is an equally acceptable root. This is in conflict with Chandrasekhar's statement that his Eq. (125) ''allows only one root whose real part is positive'' referring, no doubt, to Z_1. For $X>1$ we have $Z_2>0$; however, we find that $Z_2<1$ and therefore the associated dimensionless growth rate Y_2 is negative, indicating that this is a decaying solution, i.e., $\gamma<0$. We conclude that there is only one true growth rate given explicitly by Eq. (22).

---

[1] S. Chandrasekhar, *Hydrodynamic and Hydromagnetic Stability* (Oxford University Press, London, 1968), Chap. X.

[2] K. O. Mikaelian, Phys. Rev. E **47**, 375 (1993).

[3] R. Bellman and R. H. Pennington, Q. Appl. Math. **12**, 151 (1954).

[4] R. Hide, Proc. Camb. Philos. Soc. **51**, 179 (1955).

[5] W. H. Reid, Proc. Camb. Philos. Soc. **57**, 415 (1961).

[6] F. Quirion, M.-C. Asselin, and G. G. Ross, Chem. Soc. Rev. **23**, 275 (1994).

[7] K. O. Mikaelian, Phys. Rev. A **42**, 7211 (1990).

[8] R. Menikoff, R. C. Mjolsness, D. H. Sharp, and C. Zemach, Phys. Fluids **20**, 2000 (1977).

[9] J. V. Uspensky, *Theory of Equations* (McGraw-Hill, New York, 1948), Chap. V.